RECENT RESULTS FROM CLEO-C

P.U.E. ONYISI
Enrico Fermi Institute, University of Chicago
Chicago, IL 60637, USA

The CLEO-c experiment, running at charm threshold, has measured many charmed meson properties relevant to electroweak physics. Here I discuss results on leptonic and semileptonic decays of D mesons and measurements of hadronic decay strong phases relevant to the extraction of the CKM angle γ from B decays.

1 Introduction

The Cabibbo-Kobayashi-Maskawa (CKM) matrix is a powerful source of information on the interactions of matter and the electroweak sector of the Standard Model. Precision measurement of the CKM matrix elements relies on meson decays and properties; relating the observed hadron behavior to "short-distance" weak dynamics requires understanding the effects of the strong force. Lattice QCD offers the prospect of a systematically-improvable method of calculating hadronic properties from first principles. In the past decade theoretical and technological improvements (in particular the handling of virtual quark-antiquark pairs, the so-called "unquenched" calculations) have allowed the lattice to deliver predictions that are in many cases very precise, have no tunable parameters, and reliably estimate systematic uncertainties. Before application of these results to extract electroweak parameters in the B system, it is desirable to test them elsewhere, for example in charm.

The CLEO-c experiment at the CESR-c electron-positron collider collected large data samples in the charm threshold energy region, which enable tests of lattice predictions for charm hadron decays as well as investigations of many other topics. Here I will discuss measurements of the meson decay constant f_{D_s}, branching fractions and form factors for the semileptonic decays $D^{0,+} \to (K,\pi)e^+\nu_e$, and strong force-induced decay phases that are relevant for interferometry in the B system.

2 Detector and Data Samples

The CLEO-c detector was a symmetric general purpose detector at the CESR-c e^+e^- collider. The experiment is described in detail elsewhere.[1] The relevant datasets for the following analyses were collected at center of mass energies of approximately 3.77 GeV (the peak of the $\psi(3770)$ resonance) and 4.17 GeV. The former dataset is used for D^0 and D^+ analyses, and the latter for D_s physics. Except where noted, all analyses use the full datasets of 818 pb^{-1} at 3.77 GeV and 600 pb^{-1} at 4.17 GeV.

At 3.77 GeV the only allowed open charm final states are $D^0\overline{D}^0$ and D^+D^-; at 4.17 GeV the only allowed states involving a D_s meson are $D_s^+D_s^-$ and $D_s^\pm D_s^{*\mp}$. This enables the powerful

tagging technique pioneered by Mark III [2] which uses a fully reconstructed D meson decaying to a tag mode to indicate the presence of its antiparticle. This is the basis of the technique for measuring absolute branching fractions used in the analyses discussed below:

$$\mathcal{B}(D \to X) = \frac{N(\overline{D} \to \text{tag}, D \to X)}{N(\overline{D} \to \text{tag})} \frac{\epsilon(\overline{D} \to \text{tag})}{\epsilon(\overline{D} \to \text{tag}, D \to X)} \tag{1}$$

where the ϵ are the respective efficiencies. There are other benefits to tagging: invisible particles can be inferred from missing energy and momentum in an event; the removal of a tag's daughter particles strongly reduces the combinatorics and backgrounds of the rest of the event; and a judicious choice of D^0 tags allows the exploitation of quantum correlations of the initial state to measure phases.

3 Leptonic Decays and Decay Constants

The decays $X^+ \to \ell^+\nu$ of pseudoscalars involve a hadronic current (parametrized by the single "decay constant" f_X) and a leptonic current, which is well understood in the Standard Model. The branching fraction for such a decay can be written

$$\mathcal{B}(X^+ \to \ell^+\nu) = f_X^2 |V|^2 \frac{G_F^2}{8\pi} m_X m_\ell^2 \left(1 - \frac{m_\ell^2}{m_X^2}\right)^2 \tag{2}$$

where V is the relevant element of the CKM matrix connecting the valence quarks of X (V_{cd} and V_{cs} for D^+ and D_s^+, respectively). In a naïve quantum mechanical picture, the decay constant is a measure of the wave function of the meson at zero separation between the quarks. This means it is relevant for processes where the relevant length scales are much smaller than the hadron size, such as the loop diagrams for B_d^0 and B_s^0 mixing, which are our primary source of information on V_{td}.

Measuring the branching fraction gives $f_X^2|V|^2$; knowing the decay constant, we can obtain the CKM element, and vice versa. CLEO-c has measured the D^+ and D_s^+ decay constants in different decay modes, most recently $D_s^+ \to \tau^+\nu$ ($\tau^+ \to \rho^+\bar{\nu}$), discussed below.

3.1 $D_s^+ \to \tau^+\nu$ ($\tau^+ \to \rho^+\bar{\nu}$)

This measurement [3] requires a full reconstruction of all visible particles in the event. Nine hadronic D_s^- decays are used as tagging modes [a]. The photon from the $D_s^* \to \gamma D_s$ decay is identified by requiring the mass recoiling against the γD_s^- system to be consistent with the D_s mass. This procedure identifies 44 thousand tagged D_s events for further study.

The visible products of the D_s^+ (a π^+ and a π^0) are then reconstructed. Events with additional tracks are vetoed. Since hadrons can interact in the detector material to produce additional showers in the calorimeter, events with additional calorimeter energy are not rejected; the sum of extra energy E_{extra} should, however, be small, and this variable is used to separate signal and control samples.

To extract the signal, the mass recoiling against the reconstructed visible particles of the event (specifically, the missing mass squared MM^2) is computed. To improve the resolution, the $D_s^* \to \gamma D_s$ transition photon is associated to the D_s^- or the D_s^+ by choosing the hypothesis with a better χ^2 in a kinematic fit, and then the appropriate mass constraints are applied.

Because this decay has two neutrinos in the final state, the MM^2 variable does not peak for the signal; it instead describes a falling slope from around 0 to 0.5 GeV^2. The leading backgrounds to the signal involve the loss of one particle and so, by contrast, are peaking

[a] Charge conjugate reactions are implied.

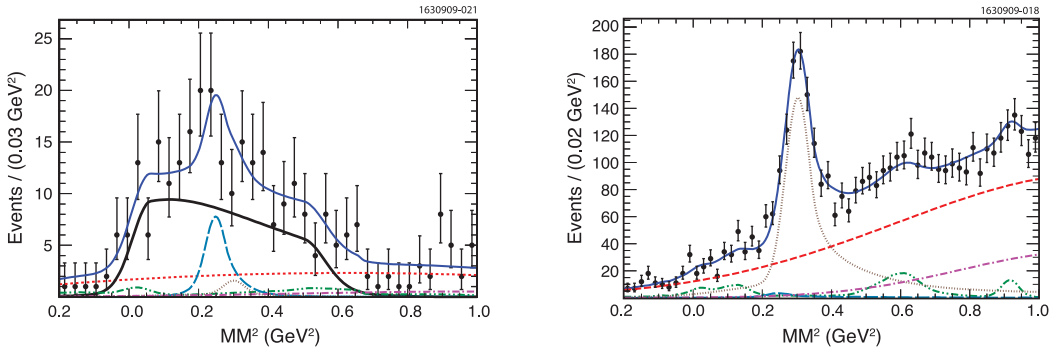

Figure 1: Missing mass squared spectra in the $\mathcal{B}(D_s^+ \to \tau^+\nu)$ analysis for different bins of extra calorimeter energy: $E_{\rm extra} < 0.1$ GeV (left) and $E_{\rm extra} > 0.8$ GeV (right). (Not shown is the spectrum for the region $0.1 < E_{\rm extra} < 0.2$ GeV.) The signal is seen in the left plot as the relatively flat black contribution from 0 to 0.5 GeV^2. The peak in the left plot at 0.25 GeV^2 is due to the $D_s^+ \to K^0\pi^+\pi^0$ background where the K^0 is not vetoed. The right plot is the control region for our modeling of backgrounds and resolution. The large peak seen in this plot is due to $D_s^+ \to \eta\rho^+$; other peaks are due to various decays with small branching fractions. The large smooth contribution rising towards the right is the contribution from fake D_s^- tags.

Table 1: CLEO-c measurements of D^+ and D_s^+ leptonic decay branching fractions and decay constants, compared to lattice QCD predictions from the HPQCD and UKQCD collaborations.

	CLEO-c Result	Lattice QCD [7]
$\mathcal{B}(D^+ \to \mu^+\nu)$ [4]	$(3.82 \pm 0.32 \pm 0.09) \times 10^{-4}$	
$\mathcal{B}(D_s^+ \to \mu^+\nu)$ [5]	$(5.65 \pm 0.45 \pm 0.17) \times 10^{-3}$	
$\mathcal{B}(D_s^+ \to \tau^+\nu)$ (from $\tau^+ \to \pi^+\bar{\nu}$) [5]	$(6.42 \pm 0.81 \pm 0.18) \times 19^{-2}$	
$\mathcal{B}(D_s^+ \to \tau^+\nu)$ (from $\tau^+ \to e^+\nu\bar{\nu}$) [6]	$(5.30 \pm 0.47 \pm 0.22) \times 10^{-2}$	
$\mathcal{B}(D_s^+ \to \tau^+\nu)$ (from $\tau^+ \to \rho^+\bar{\nu}$) [3]	$(5.30 \pm 0.47 \pm 0.22) \times 10^{-2}$	
f_{D^+}	$205.8 \pm 8.5 \pm 2.5$ MeV	207 ± 4 MeV
$f_{D_s^+}$ (combined)	$259.0 \pm 6.2 \pm 3.0$ MeV	241 ± 3 MeV

structures. The background modeling is validated by looking at events with $E_{\rm extra} > 0.8$ GeV; the signal is then extracted separately in the bins $E_{\rm extra} < 0.1$ GeV and $0.1 < E_{\rm extra} < 0.2$ GeV. The background contributions from different sources are allowed to float in these fits and the results are in good agreement with Monte Carlo expectations. The fits for $E_{\rm extra} < 0.1$ GeV and $E_{\rm extra} > 0.8$ GeV are shown in Figure 1. A clear signal is observed allowing for extraction of the branching fraction and decay constant.

The results of all CLEO-c leptonic branching fraction measurements and the corresponding decay constants are shown in table 1. The values of input parameters used to obtain these values are listed in the relevant papers.[3,4,5,6]

4 Exclusive Semileptonic Decays

Exclusive semileptonic decays have a more involved parametrization than leptonic decays, as there are at least three particles in the final state. The partial width for the decay $X \to X'\ell\nu$, where X and X' are pseudoscalars, can be written as

$$\frac{d\Gamma(X \to X'\ell\nu)}{dq^2} = \frac{G_F^2}{24\pi^3}\left[f_+^{X\to X'}(q^2)|V|\right]^2 p_{X'}^3 \qquad (3)$$

in the limit where the charged lepton mass is negligible. In eq. 3, q^2 is the invariant mass squared of the $\ell\nu$ system, $|V|$ is the relevant CKM matrix element for the weak transition, and $f_+^{X\to X'}$

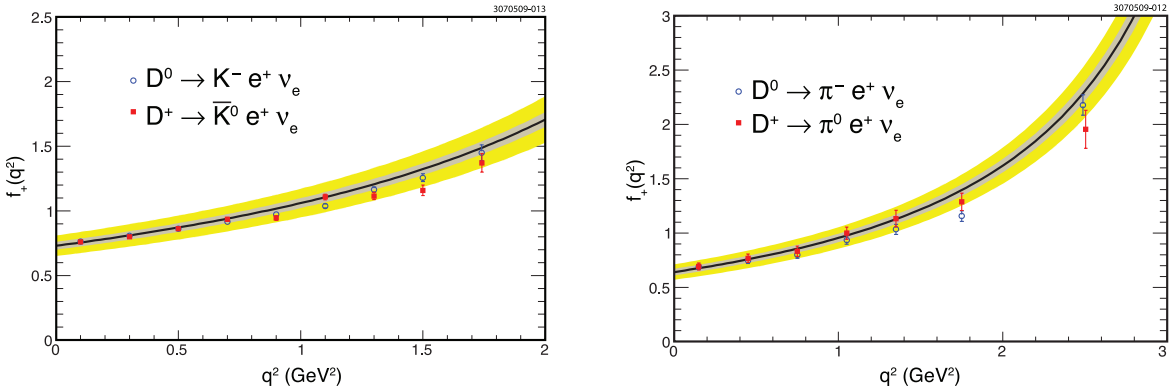

Figure 2: D semileptonic decay form factors for kaon (left) and pion (right) decays as a function of q^2. The points are CLEO-c data; the bands are from a lattice QCD prediction.

is a form factor encapsulating the hadronic physics. As in the leptonic decay case, input for $|V|$ or f_+ allows determination of the other.

The analysis [8] of $D \to (K,\pi)e^+\nu$ reconstructs hadronic decays of one D in the event to establish the base sample. A hadron ($K^\pm$, $\pi^\pm$, K^0_S, π^0) and an electron candidate are then selected, and the missing energy E_{miss} and momentum $\vec{p}_{miss}$ are determined. The variable $U \equiv E_{miss} - |\vec{p}_{miss}|$ is computed, which peaks at zero for correctly reconstructed signal events. Events with additional particles, or where the hadron has been wrongly reconstructed, are strongly separated from zero in U.

The yields as a function of q^2 are used to derive measurements of the form factors. These are fit to several parametrizations: the simple pole model assuming D_s^*/D^* dominance, the "modified pole" model,[9] and a series expansion.[10] All fits describe the data reasonably as long as all parameters are allowed to float; however the implied D_s^*/D^* masses in the pole models are many standard deviations from the physical values. Reasonable agreement on the form factor shape and normalization is found with a lattice QCD prediction from the FNAL, MILC, and HPQCD collaborations;[11] a comparison can be seen in Figure 2. Using lattice predictions for $|f_+(0)|$, values for $|V_{cd}|$ and $|V_{cs}|$ are also obtained, which are limited by lattice uncertainties.

5 Strong Phases for γ/ϕ_3 Measurements

Of the three angles of the unitarity triangle, γ has the largest uncertainties on its direct measurement. A clean measurement of γ from tree decays can be made by exploiting interference between the decays $b \to c\bar{u}s$ and $b \to u\bar{c}s$. These correspond to decays $\overline{B} \to DK$ and $\overline{B} \to \overline{D}K$, which interfere when D^0 and $\overline{D}^0$ decay to common final states. Such final states include $K^-\pi^+$ (interference between Cabibbo-favored and doubly-Cabibbo-suppressed decays) [12] and $K^0_S\pi^+\pi^-$ (Cabibbo-favored in both cases, but populating different parts of phase space).[13] The total observed interference depends on D decay dynamics — specifically strong force-induced phases between D and $\overline{D}$ decays to the same final state. As B-factories observe definite flavor in D^0 decays (as they tag the soft pion in $D^{*+} \to D^0\pi^+$), they cannot directly observe these phases. In the case of decays to common three-body final states, the phases can be estimated by using models for the resonant substructure of the decays, but this leaves a residual model uncertainty.

Production of $D^0\overline{D}^0$ pairs at threshold provides unique access to the phase information. The initial state is strongly constrained ($J^{PC} = 1^{--}$) and so the decays of the two D mesons are correlated. One obvious correlation is flavor-antiflavor (in the absence of mixing); a less obvious one is CP correlation: if one D decays to a CP eigenstate (for example K^-K^+), the other must decay to a state of opposite CP. This projects out a linear sum of the D^0 and $\overline{D}^0$

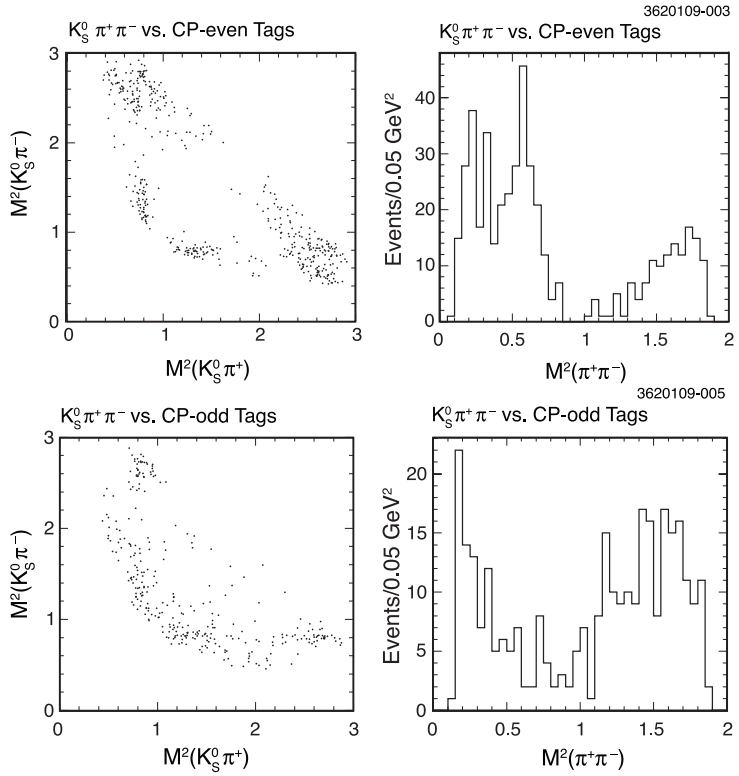

Figure 3: Effects of CP correlation on the Dalitz plot of the decay $D^0 \to K^0_S\pi^+\pi^-$. The $K^0_S\rho^0$ component, clearly visible when $K^0_S\pi^+\pi^-$ recoils against a CP-even tag, disappears opposite a CP-odd tag.

flavor eigenstates, which interfere. Comparing the rates and dynamics of the same decay when it happens opposite flavor and CP eigenstates directly probes the strong phases in D^0 decays without model systematics. The dramatic effect of these correlations is shown in Figure 3.

Here I summarize CLEO-c results relevant to γ measurements.

5.1 Strong Phase Between $D^0 \to K^-\pi^+$ and $\overline{D}^0 \to K^-\pi^+$

The relative phase δ between the decays $D^0 \to K^-\pi^+$ and $\overline{D}^0 \to K^-\pi^+$ is relevant for the γ measurement method of Atwood, Dunietz, and Soni.[12] This phase also relates the D^0 mixing parameters y and y'. The differences in the effective branching fraction for $K^-\pi^+$ decay opposite CP-even and -odd eigenstates, semileptonic decays (which unambiguously determine the charge of the decaying charm quark), and $K^+\pi^-$ are sensitive to δ and in principle to D^0 mixing parameters as well. With 281 pb^{-1} of data, CLEO-c has made the first measurement $\cos\delta = 1.03^{+0.31}_{-0.17} \pm 0.06$.[14]

5.2 Effective Strong Phases In Multibody Decays

The γ measurement method using $K^-\pi^+$ decays can be extended to other decays with larger branching fractions.[15] In this case the relative phase depends on the decay kinematics, and the Cabibbo-favored and doubly-Cabibbo-suppressed decays will not have complete overlap over the phase space. These effects can be described by an effective average phase and a "coherence factor" which reflects the dilution of total interference relative to a simple two-body decay. CLEO-c has measured these for the $D^0 \to K^-\pi^+\pi^0$ and $K^-\pi^+\pi^+\pi^-$ decays, observing significant coherence in the former.[16]

5.3 Phase Space-Dependent Measurements

Beyond the averaging approximation above, we can obtain relative D^0–$\overline{D}^0$ phases as a function of decay kinematics by observing how CP tagging affects Dalitz plots. CLEO-c has performed this measurement for the $K^0_{S,L}\pi^+\pi^-$ decay [17] and work is underway for the $K^0_{S,L}K^-K^+$ mode. Figure 3 shows the effect of the CP correlations on the $D^0 \to K^0_S\pi^+\pi^-$ Dalitz plot. Even though only the K^0_S modes are relevant for B factory measurements, CLEO-c can reconstruct K^0_L candidates using missing energy and momentum and improve its measurements, as up to small effects $K^0_L\pi^+\pi^-$ has a CP structure opposite that of $K^0_S\pi^+\pi^-$.

5.4 Impact on γ Measurement

The impact of CLEO-c results on future analyses enabled by the large dataset expected from LHCb has been studied by the LHCb Collaboration. The $D^0 \to K^0_S\pi^+\pi^-$ analysis is expected to reduce the current 7–9° model uncertainties from BaBar and Belle measurements [18] to around $2°$.[17,19] The $K^-\pi^+$ and multibody coherence factor measurements are projected to improve the 10 fb^{-1} precision of LHCb in $B \to DK$ by 8–35% (depending on unknown B decay parameters) to 2.2–3.5°.[20]

Acknowledgments

This work was partly supported by a Fermi Fellowship from the University of Chicago.

1. Kubota Y. *et al.*, *Nucl. Instrum. Meth. Phys. Res., Sect. A* **320**, (1992) 66; Peterson D. *et al.*, *Nucl. Instrum. Meth. Phys. Res., Sect. A* **478**, (2002) 142; Artuso M. *et al.*, *Nucl. Instrum. Meth. Phys. Res., Sect. A* **554** (2005), 147.
2. Baltrusaitis R. M. *et al.*, *Phys. Rev. Lett.* **56**, (1986) 2140; Adler J. *et al.*, *Phys. Rev. Lett.* **60**, (1988) 89.
3. Naik P. *et al.*, *Phys. Rev. D* **80**, (2009) 112004.
4. Eisenstein B. I. *et al.*, *Phys. Rev. D* **78**, (2008) 052003.
5. Alexander J. P. *et al.*, *Phys. Rev. D* **79**, (2009) 052001.
6. Onyisi P. U. E. *et al.*, *Phys. Rev. D* **79**, (2009) 052002.
7. Follana E. *et al.*, *Phys. Rev. Lett.* **100**, (2008) 062002.
8. Besson D. *et al.*, *Phys. Rev. D* **80**, (2009) 032005.
9. Becirevic D. and Kaidalov A. B., *Phys. Lett. B* **478**, (2000) 417.
10. Becher T. and Hill R. J., *Phys. Lett. B* **633**, (2006) 61.
11. Aubin C. *et al.*, *Phys. Rev. Lett.* **94**, (2005) 011601.
12. Atwood D., Dunietz I., and Soni A., *Phys. Rev. Lett.* **78**, (1997) 3257.
13. Giri A. *et al.*, *Phys. Rev. D* **68**, (2003) 054018; Bondar A. and Poluektov A., *Eur. Phys. J. C* **47**, (2006) 347.
14. Rosner J. L. *et al.*, *Phys. Rev. Lett.* **100**, (2008) 221801.
15. Atwood D. and Soni A., *Phys. Rev. D* **68**, (2003) 033003.
16. Lowery N. *et al.*, *Phys. Rev. D* **80**, (2009) 031105.
17. Briere R. A. *et al.*, *Phys. Rev. D* **80**, (2009) 032002.
18. Aubert B. *et al.*, *Phys. Rev. D* **78**, (2008) 034023; Abe K. *et al.*, arxiv:0803.3375 (2008).
19. Libby J., CERN-LHCb-2007-141, 2007, unpublished.
20. Akiba K. *et al.*, CERN-LHCb-2008-031, 2008, unpublished.